Biochimica et Biophysica Acta, 945 (1988) 73–80
Elsevier

BBA 74179

ESR studies on the ripple phase in multilamellar phospholipid bilayers

Kazuaki Tsuchida [a] and Ichiro Hatta [b]

[a] *Department of Physics, Suzuka College of Technology, Shirokocho, Suzuka,* and [b] *Department of Applied Physics, Nagoya University, Chikusaku, Nagoya (Japan)*

(Received 20 June 1988)

Key words: Dipalmitoylphosphatidylcholine; Phase transition; Ripple structure; ESR

The structure of the ripple phase in multilamellar DPPC liposomes was studied by measuring electron spin resonance (ESR) spectra of the stearic acid spin probe (16-SASL). The spectrum observed in the $P_{\beta'}$ phase is explained in terms of the superposition of ordered- and disordered-type spectra. This fact suggests the existence of a nonhomogeneous structure in the $P_{\beta'}$ phase, i.e., the coexistence of the ordered region present in the $L_{\beta'}$ phase and the disordered region present in the L_α phase. The fluidity of acyl chains in both regions and the intensity ratio of the disordered-type spectra to the total intensity were estimated from the ESR spectra at various temperatures. The fluidity of both regions did not exhibit remarkable temperature dependence. On the other hand, the intensity ratio showed almost similar temperature dependence of the partitioning of the TEMPO observed by ESR measurement and of the enthalpy curve by DSC measurement, that is, the intensity ratio value increases slowly near the pretransition temperature, is almost constant in the $P_{\beta'}$ phase, and increases abruptly at the main transition temperature with temperature. The proportion of the disordered region is estimated to be about one-fifth to the total region in the $P_{\beta'}$ phase. Based upon the above results, a model for the ripple structure is proposed.

Introduction

Electron spin resonance (ESR) spectroscopy of fatty acid spin labels had widely been used to investigate the motion of acyl chains in lipid bilayers and biological membrane [1,2]. In this study, a 'order parameter', which characterizes the degree of the wobbling motion of acyl chains, has been considered. Hubbell and McConnell [1] have revealed that the wobbling motion of acyl chain becomes more vigorous as the position is apart from the phosphatidylcholine head group. It has been reported in various phospholipids that the order parameter decreases abruptly at the main transition temperature T_m with temperature in connection with the chain melting [3,4]. However, the motional state of acyl chains in the $P_{\beta'}$ phase below T_m has not been clarified in detail yet.

Recently, Wittebort et al. [6] have investigated the ^{13}C-NMR spectra of DPPC in the $P_{\beta'}$ phase. The result indicates that the spectrum is composed of the superposition of two spectra associated with the $L_{\beta'}$ and the L_α phases. They have pointed out therefore that the structure of the $P_{\beta'}$ phase possesses the nature of both the $L_{\beta'}$ and the L_α

Abbreviations: DPPC, dipalmitoylphosphatidylcholine; DMPC, dimyristoylphosphatidylcholine; ESR, electron spin resonance; DSC, differential scanning calorimetry; 5-SASL, 2-(3-carboxypropyl)-4,4-dimethyl-2-tridecyl-3-oxazolidinyloxyl; 12-SASL, 2-(10-carboxydecyl)-2-hexyl-4,4-dimethyl-3-oxazolidinyloxyl; 16-SASL, 2-(14-carboxytetradecyl)-2-ethyl-4,4-dimethyl-3-oxazolidinyloxyl; TEMPO, 2,2,6,6-tetramethylpiperidine-*N*-oxyl.

Correspondence: K. Tsuchida, Department of Physics, Suzuka College of Technology, Shirokocho, Suzuka 510-02, Japan.

phases. Falkovitz et al. [7] have proposed a new model for the structure of the $P_{\beta'}$ phase from a theoretical consideration using a Landau-De Gennes free energy for phospholipid bilayers. The analysis to minimize the energy leads to a model for the structure in the $P_{\beta'}$ phase, which has undulated surface and periodic variation of the fluidity. Schneider et al. [8] have investigated the diffusion of a fluorescent lipid in the $P_{\beta'}$ phase of DMPC. They have reported that the diffusion in this phase is dominated by fast diffusion along banded structure and have concluded that this diffusion originates from the disordered region associated with the ridges or their furrows in the ripple structure. They have also proposed a model for the $P_{\beta'}$ phase with the periodic variation of the fluidity.

Based upon the above feature, we can proceed the study on the detailed feature of the motional state of acyl chains in the phospholipid bilayers and the structure of the $P_{\beta'}$ phase. In the present experiment, the stearic spin probes are used for studyng the motion of acyl chains in multilamellar DPPC. The detailed temperature dependence of the ESR spectra is observed and then analyzed in terms of the superposition of the spectra for the ordered and the disordered regions near and below T_m. Then, the intensity ratio between the ordered- and the disordered-type spectra is obtained as a function of temperature. Finally, from the present experimental results, a plausible model of the ripple structure in the $P_{\beta'}$ phase is proposed.

Experimental procedure

L-α-Dipalmitoylphosphatidylcholine (DPPC) which was more than 99% pure was purchased from Sigma Chem. Co. and stearic acid spin probes, 2-(14-carboxytetradecyl)-2-ethyl-4,4-dimethyl-3-oxazolidinyloxyl (16-SASL), 2-(10-carboxydecyl)-2-hexyl-4,4-dimethyl-3-oxazolidinyloxyl (12-SASL) and 2-(3-carboxypropyl)-4,4-dimethyl-2-tridecyl-3-oxazolidinyloxyl (5-SASL) were purchased from Aldrich Chem. Co. The purity of DPPC was established by thin-layer chromatography. The phospholipid was dissolved in chloroform and a stearic acid spin probe (0.5 mol%) was added to the phospholipid solution. The solvent was evaporated under the stream of nitrogen gas. The remaining phospholipid was treated overnight in evacuated desiccator to remove residual solvent. Finally distilled water was added to the phospholipid. The concentration of the phospholipid to water was 30 wt%. This sample was kept at 50 °C for an hour, vortexed with glass beads for 5 min at 50 °C to obtain a homogeneous suspension and put into a sample tube for ESR experiment. The pH of the suspension was 6.4. A small sample tube was used in order to exclude the temperature gradient in the sample. The size of the sample cell was 1.4 mm in diameter and 2.0 mm in length. The calibrated copper-constantan thermocouple was set in the center of the sample to measure the temperature directly, which was controlled by blowing nitrogen gas with the accuracy of ± 0.05 °C. The temperature inhomogeneity in the sample was within 0.05 °C. The ESR spectra were measured at the frequency of an X-band with a ESR spectrometer (JEOL FE1X). Three types of stearic acid spin probes, 16-SASL and subsidiarily 12-SASL and 5-SASL, were used. Qualitatively similar tendency was obtained for these three probes. The results for mainly 16-SASL will be discussed, since the spectrum of 16-SASL gives clearer splitting into the two distinct spectra for ordered and disordered states than that of the other probes in the $P_{\beta'}$ phase.

Result

The ESR experiment of the stearic acid spin labels in the multibilayers provides us fruitful information about the motion and/or the order of acyl chains in membranes [1–4]. In the most membranes, rapid rotational motion of the probes around the acyl chains leads to an axially symmetric effective spin Hamiltonian with the parameters of hyperfine tensor, $T_{\parallel}$ and $T_{\perp}$, and g tensor, $g_{\parallel}$ and $g_{\perp}$, where the subscripts indicate parallel and perpendicular to the symmetry axis, respectively. The order parameter is defined as

$$S = \frac{T_{\parallel} - T_{\perp}}{T_{\parallel}^{\circ} - T_{\perp}^{\circ}} \tag{1}$$

where $T_{\parallel}^{\circ}$ and $T_{\perp}^{\circ}$ are the values expected in the ordered-chains, approx. 33 and 6 gauss for a

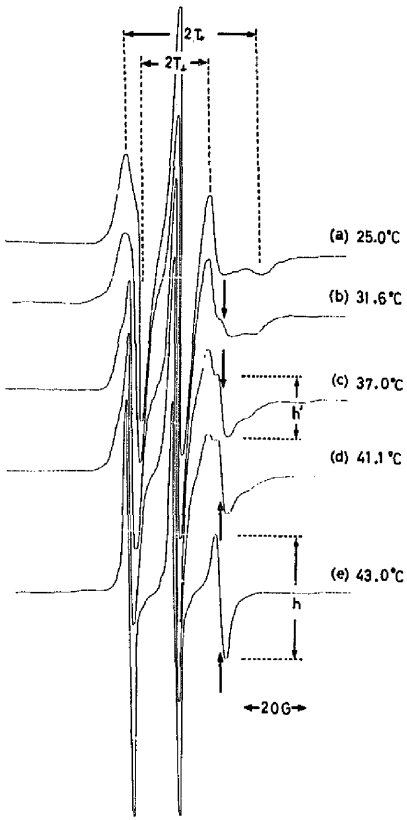

Fig. 1. Temperature dependence of the ESR spectra of 16-SASL in the multilamellar DPPC liposomes. The resonance lines corresponding to the disordered state of acyl chains are shown by solid arrows.

nitroxide radical, respectively. Since the order parameter decreases as the wobbling motion becomes vigorous, the order parameter well represents the degree of the motion of acyl chains. Figs. 1a to e show the ESR spectra of 16-SALS in the multilamellar DPPC liposome at various temperatures. In the multilamellar liposome, ESR spectrum results from the sum of the spectra of various oriented bilayers. Fig. 1a indicates a representative ESR spectrum of 16-SASL in the $L_{\beta'}$ phase. In the spectrum of the multilamellar liposome, usually the hyperfine parameters, $T_{\parallel}$ and $T_{\perp}$, have been measured approximately as denoted in Fig. 1a. These parameters were, however, determined by the simulation method in the present experiment. Fig. 1e is a representative spectrum in the L_{α} phase, the order parameter of which is smaller than 0.1. It should be pointed out that the spectrum of the L_{α} phase is observed even in the $P_{\beta'}$ phases, whose resonance lines are indicated by arrows in Figs. 1b–1e. Although this spectrum grows near the pretransition temperature, its intensity does not show remarkable change in the $P_{\beta'}$ phase. The ESR spectra shown in Figs. 1b–d is not explained by a single-order parameter, but can be interpreted in terms of superposition of two types of spectra.

It is well known that the protonated and unprotonated forms of the spin-labelled fatty acids often give rise to the two component ESR spectra [9,10]. The superposition of the spectra in the present experiment is, however, not due to the two forms of the label, as will be discussed in the Discussion. Therefore, it is certainly concluded that the state of acyl chains is not homogeneous in the $P_{\beta'}$ phase, that is, the two regions coexist in the $P_{\beta'}$ phase. The motional state of acyl chains is the same as in the $L_{\beta'}$ phase in one region and the same as in the L_{α} region in the other region, which we call ordered and disordered region in the present paper, respectively. The spectra near the main transition temperature T_m are magnified in Fig. 2. The intensity of the disordered-type spectra whose resonance lines are indicated by solid arrows increases abruptly at T_m with temperature and conversely that of the ordered-type spectra whose resonance lines are indicated by dotted arrows decreases at T_m with temperature. On the other hand, the position of the resonance peaks shown by arrows in Fig. 2 does not exhibit any remarkable change.

We tried to analyze these spectra. In this analysis, the rotational and wobbling motion of the stearic acid spin probes are assumed to be in the fast motional regime. The line shapes of this regime are discussed in various review articles [11,12]. The spectra were fitted in terms of the weighted sums of two spectra which had the different order parameters of acyl chains; S^{L} and S^{H} for the ordered and the disordered regions, respectively. The spin Hamiltonian parameters of ordered-type spectra, $T_{\parallel}^{L}$ and $T_{\perp}^{L}$, are deduced from Eqn. 1, using the order parameter S^{L} and the parameters $T_{\parallel}^{o}$ and $T_{\perp}^{o}$ together with the iso-

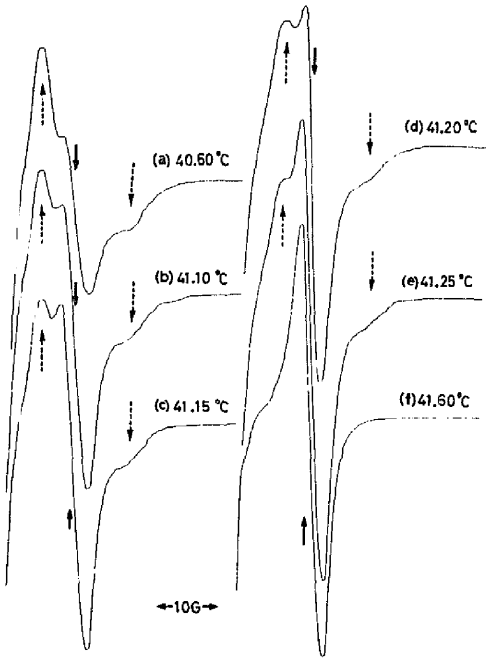

Fig. 2. The temperature dependence of the ESR spectra near T_m. The high magnetic field parts of the ESR spectra of Fig. 1 are magnified. The solid and dotted arrows denote the resonance lines corresponding to disordered- and ordered-type spectra, respectively.

tropic part of the hyperfine interaction $T_{iso} = (T_{\parallel} + 2T_{\perp})/3$

$$T_{\parallel}^{L} = T_{iso} + \tfrac{2}{3}(T_{\parallel}^{o} - T_{\perp}^{o})S^{L} \quad (2)$$

$$T_{\perp}^{L} = T_{iso} - \tfrac{1}{3}(T_{\parallel}^{o} - T_{\perp}^{o})S^{L} \quad (3)$$

Likewise the g-values, $g_{\parallel}^{L}$ and $g_{\perp}^{L}$ are deduced

$$g_{\parallel}^{L} = g_{iso} + \tfrac{2}{3}(g_{\parallel}^{o} - g_{\perp}^{o})S^{L} \quad (4)$$

$$g_{\perp}^{L} = g_{iso} - \tfrac{1}{3}(g_{\parallel}^{o} - g_{\perp}^{o})S^{L} \quad (5)$$

The parameters for disordered-type spectra, $T_{\parallel}^{H}$, $T_{\perp}^{H}$, $g_{\parallel}^{H}$ and $g_{\perp}^{H}$ are given by equations similar to Eqns. 2–5 using the parameters with the subscript H instead of L. The values of $T_{\parallel}^{o}$ and $T_{\perp}^{o}$ are determined in the following way. Although the principal values of hyperfine tensor in stearic acid spin probes, T_{xx}, T_{yy} and T_{zz}, have been determined precisely in the single crystal [13], these values should be corrected by taking into account the polarity of the medium where the spin label is located [11,12]. This correction is done by multiplying them by a constant factor k: $T'_{xx} = kT_{xx}$, $T'_{yy} = kT_{yy}$, $T'_{zz} = kT_{zz}$ and $T'_{iso} = (T'_{xx} + T'_{yy} + T'_{zz})/3 = kT_{iso}$, where the dashed values are those in the present sample. The principal values of the g tensor are corrected in the same way. Since the hyperfine tensor was almost isotropic in the L_α phase as shown in Fig. 1e, the T_{iso} was obtained from the spectrum in the L_α phase and then the value of k was estimated. Consequently, the following values were adopted for the perfectly ordered chains; $T_{\parallel}^{o} = kT_{zz} = 32.9$, $T_{\perp}^{o} = k\ (T_{xx} + T_{yy})/2 = 5.8$ in gauss, and in the same way $g_{\parallel}^{o} = 2.0026$ and $g_{\perp}^{o} = 2.0073$. The ratio of the spectral intensity for labels in the disordered regions to the intensity for the total labels was defined by P. The ESR spectra were calculated by the following way. The Lorentzian lines shapes with the width of 2.5 gauss were used and were summed for all directions according to multilamellar liposomes. The ordered- and disordered-type spectra were calculated for various values of S^{L} and S^{H}. These spectra were superposed by varying the value of P in order to find the best-fitted curves. Fig. 3 shows an example of the fitted curve to the observed one at 37.5 °C with the values, $S^{L} = 0.40$, $S^{H} = 0.09$ and $P = 0.23$. This figure indicates that the experimental data are well explained in the spectra based on the coexistence of two regions. Since the disordered-type lines are sharp, this spectrum looks to be dominant in Fig. 3 at a first glance. It is revealed, however, from the analysis that the ordered-type spectrum (shown by the dotted arrows) is about three times as intense as the disordered-type spectrum (indicated by the solid arrows). The above procedure of simulation was carried out for the spectra at various temperatures. The parameters thus determined are plotted in both Figs. 4 and 5 as a function of temperature. The order parameters of the two regions, S^{L} and S^{H}, both gradually decrease with temperature and do not show a remarkable change near T_m except for the disappearance of S^{L} above T_m. On the other hand, the intensity ratio of the disordered-type spectra, P, increases abruptly at the main transition temperature as shown in Fig. 5. This exhibits the almost similar temperature depen-

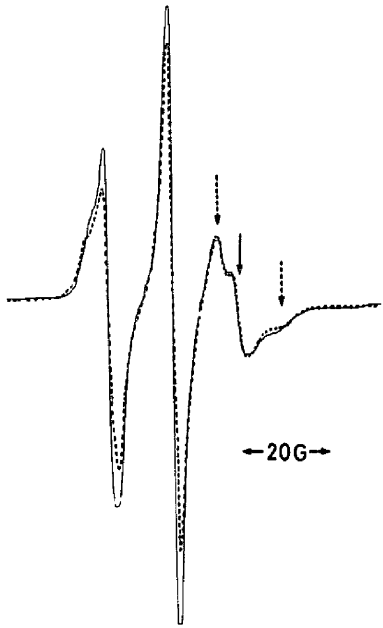

Fig. 3. Reproduced curve of the ESR spectrum at 37.5 °C. The dotted curve shows the reproduced curve with the parameters; $P = 0.23$, $S^L = 0.40$ and $S^H = 0.09$. The solid and dotted arrows indicate the resonance lines corresponding to disordered- and ordered-type spectra, respectively.

dence of the enthalpy curve in the DSC experiment [14] and of the TEMPO parameter in the ESR measurement [15]. The present results suggest that the following feature of phase transition takes place in the phospholipid bilayers; the dis-

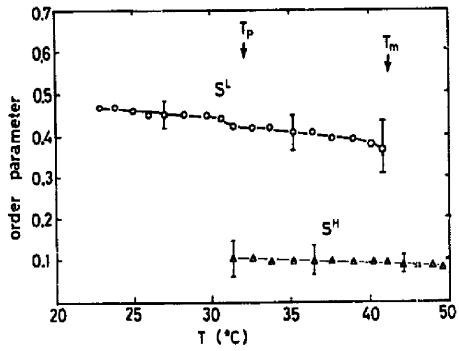

Fig. 4. Temperature dependence of the order parameters. S^L and S^H are the order parameters of acyl chains in the ordered and disordered regions, respectively.

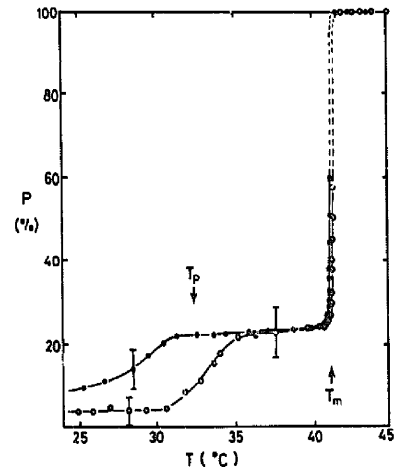

Fig. 5. Temperature dependence of P; the ratio of the intensity of the disordered-type spectrum to that of the whole spectrum. ○, on heating; ●, on cooling.

ordered regions exist even in the $P_{\beta'}$ phase, in which the order parameter of acyl chains S^H is almost the same as in the L_α phase as shown in Fig. 4; the area occupied by this region is almost constant over the $P_{\beta'}$ phase as shown in Fig. 5; this area grows up abruptly at T_m (see Fig. 5) and almost all chains become disordered in the L_α phase (see Fig. 4).

It might be queried whether the ratio of the spectral intensity, P, is just the same as the ratio of the disordered area to the whole surface. If the density of the probes in the disordered region is higher than that in the ordered region as in the case of TEMPO spin probes, then the ratio P does not directly reflect the ratio of the disordered region. The quantitative estimation of the disordered area is discussed in the following section.

Discussion

The spin-labelled fatty acids often give rise to the two component ESR spectra due to the protonated and unprotonated form of the probes. In relation to this fact, the ESR spectra of methyl ester of 16-SASL, 2-(14-carboxytetradecyl)-2-ethyl-4,4-dimethyl-3-oxazolidinyloxyl methyl ester, were also measured, which is expected to give the spectra for only protonated form. The ESR

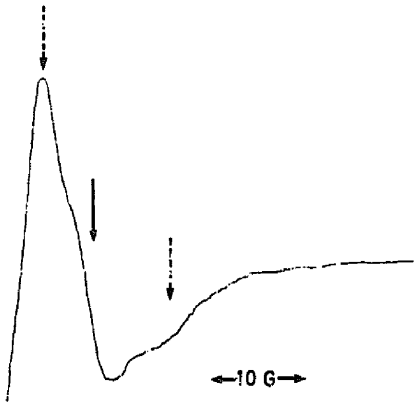

Fig. 6. The high magnetic field part of the ESR spectrum of the ester of 16-SASL at 37.5°C. The solid and dotted arrows indicate the resonance lines corresponding to the disordered- and ordered-type spectra, respectively.

spectrum of this probes is shown in Fig. 6. The superposed spectrum almost same as that of 16-SASL is observed in the $P_{\beta'}$ phase, although the splitting is not so clear as in the case of 16-SASL. The temperature dependence of the spectrum is almost the same as that of 16-SASL, that is, the disordered-type spectrum shown by solid arrow grows at the pretransition temperature T_p and the intensity is almost constant in the $P_{\beta'}$ phase and increases abruptly at T_m. The spectra were analyzed by the same method as that for 16-SASL. The parameters determined by the simulation method were $P = 0.22$, $S^L = 0.34$ and $S^H = 0.08$ at 37.5°C. The ratio P is almost the same as that of 16-SASL in the Results. This fact indicates that the two components of the ESR spectra are not due to the difference between the protonated and unprotonated forms of the labels and that the value of P is little affected by the protonation states of the probes.

In the previous section, it was found that the intensity ratio of the disordered-type spectrum was 23% to the total intensity in the $P_{\beta'}$ phase. The real ratio of the disordered area might be smaller than the above value. The reason is that the labels in the disordered region are more concentrated than those in the ordered region. Thus, the ratio of the disordered region should be considered carefully. The unbalance of the label density between two regions was estimated in the following way. The ESR spectra in the $P_{\beta'}$ and the L_α phase were observed with various concentration of the spin probes from 0.02 to 10 mol%. Buffered suspensions (pH 6.4) were used in order to prevent any change in pH. The same spectra and temperature dependence as shown in Figs. 1 and 2 were observed in the samples in which the concentration of the probes is from 0.02 to 1.0 mol%. The solid line in Fig. 7 shows the concentration dependence of h denoted in Fig. 1e; the height of the line in the higher magnetic field in the L_α phase. The dotted line in this figure shows the concentration dependence of h' defined in Fig. 1c; which corresponds to the height of the disordered-type line in the $P_{\beta'}$ phase. The height divided by the concentration of the probes is shown in Fig. 7 and is normalized to 1 at the lowest concentration. The height h' could not be measured in samples with concentrations above 4 mol% because of the exchange broadening of lines. If the density of labels is higher in the disordered region than in the ordered region in the $P_{\beta'}$ phase, the exchange broadening takes place at the lower concentration in the disordered-type line in the $P_{\beta'}$ phase than in the L_α phase. The height in the L_α phase shows the decrease above 0.2 mol%, which is due to the exchange broadening. The height of the disordered-type line in the $P_{\beta'}$ phase shows almost same concentration dependence but begins to decrease at a little lower concentration than that in the L_α phase. Consequently, it is estimated

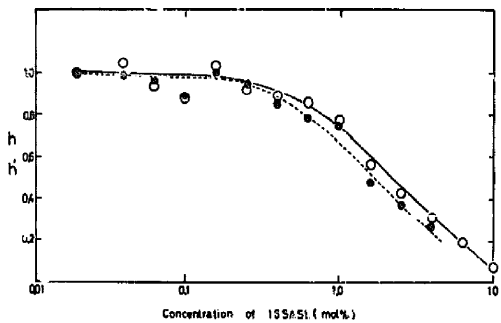

Fig. 7. The height h (○) and h' (●) at various concentration of 16-SASL. h is the height of the line in higher magnetic field in the ESR spectra of L_α phase as shown in Fig. 1e, and h' is that of the disordered-type line in the $P_{\beta'}$ phase as shown in Fig. 1c. Both heights are devided by the concentration of the probes and normalized to 1 at the lowest concentration.

from Fig. 7 that the probe density in the disordered area is about 20% higher than that in the ordered region. From this consideration and together with the intensity ratio of the spectra (23%) in the previous section, it can be concluded that the ratio of the disordered area is about one-fifth of the whole surface in the $P_{\beta'}$ phase.

In the analysis of the ESR line shape, the rotational and wobbling motion of the acyl chains in the stearic acid spin labels are assumed to be in the fast-motional regime. The ESR spectra of fatty acid spin labels which lie in the slow-motional regime have often been observed in the oriented phospholipid bilayer [4]. In the slow-motional regime, the spectrum becomes powder-like and the hyperfine splitting should have the component of the rigid acyl chain: $T_{\parallel} = T_{\parallel}^{\circ}$ (about 33 gauss) [4,16]. This component does not appear in Figs. 1a or 1e. Moreover, the spectrum of Figs. 1a and 1e are approximately analyzed by using the labels in the fast-motional limit. These facts indicate that the motion of 16-SASL in the present experiment are almost in the fast motional regime. Although the contribution from the slow motional effect are not evident in the unoriented phospholipid bilayer [4], the line shape might be somewhat influenced by this slow-motional contribution. Then, it should be noted that the present order parameters are the effective values which might more or less contain the contribution from the slow-motional effect of acyl chains.

In the present experiment, almost all spectra were well represented in terms of the superposition of two types of spectra in the case of 16-SALS. This result draws that the ordered and disordered regions coexist in the $P_{\beta'}$ phase. This is consistent with the NMR experiment [6,17], the fluorescent measurement [8,18] and the theoretical consideration [7]. The temperature dependence of the intensity of the disordered-type spectra and that of the order parameters in the both regions were analyzed quantitatively by the simulation of the ESR spectra. Consequently, the temperature dependence of the TEMPO parameter and the enthalpy curve by DSC experiment can be interpreted within the framework of the present model.

Together with the ESR spectra of 16-SASL, those of 5-SASL and 12-SASL were subsidiarily measured. The same simulation as that for 16-SASL in the previous section was also performed. Since the splitting of the two types of spectra is not so clear as in Figs. 1 and 2, the parameters could not be determined as accurately as in the case of 16-SASL It may safely be said that the spectra of 5-SASL and 12-SASL in the $P_{\beta'}$ phase could not be explained by one order parameter, and the spectra seem to be composed of the superposition of two types of spectra as in the case of 16-SASL.

In previous experiments, we studied the relaxation process at the pretransition in the multilamellar DPPC liposomes, using ESR experiment of TEMPO spin probes [19] and freeze-fracture electronmicroscopy [20]. On the temperature jump from 38°C ($P_{\beta'}$ phase) to 30°C ($L_{\beta'}$ phase), the ripple structure disappears gradually with a life time of several tens of minutes. In the present experiment, the time dependence of the ratio P was tentatively measured with the same temperature jump. The time dependence of the ratio has also the same relaxation time. These results indicates that the disordered area are almost proportional to the number of the ripples. Therefore, this suggests that the disordered regions might exist along ridges or furrows of ripples [7,8,18,21]. In the fluorescent measurement [8], the fast diffusion of a fluorescent lipid along the banded structure also suggests that this region lies along ripples. Considering the various possibility for the location of the disordered region in the phospholipid bilayer of the $P_{\beta'}$ phase, a plausible arrangement of acyl chains in the $P_{\beta'}$ phase are schematically drawn as shown in Fig. 8. Wiggly lines represent melted hydrocarbon chains and rather straight lines correspond to ordered chains. The reason

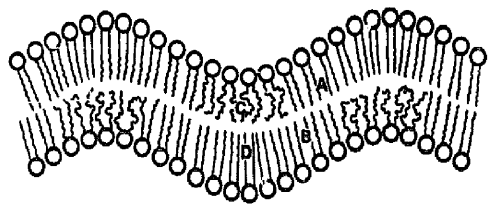

Fig. 8. A schematic view of the plausible arrangement of acyl chains in the $P_{\beta'}$ phase in the multilamellar phospholipid. The circle represents the head group. The wiggly line represents the melted hydrocarbon chain and the rather straight part corresponds to the ordered hydrocarbon chains.

why we propose this model is as follows. It is possible that the existence of the disordered regions is closely related to the bending nature of lipid bilayer caused by the rippling in the $P_{\beta'}$ phase. Although the bilayer surface has a large curvature in the regions denoted C or D in Fig. 8, the surrounding of acyl chains has opposite characteristic between the regions C and D. The recent ESR study employing biradical probes [22] indicates that the acyl chains orient perpendicular to the local (rippled) bilayer surface in the $P_{\beta'}$ phase. In the region denoted C, the density of the acyl chains is apt to become sparse, because the upper layer has a concave curvature and the surface density of the phosphatidylcholine head group remains almost unchanged. Then, acyl chains in this region are movable and therefore it is inferred that region C is likely to be disordered. It is plausible that the bilayer of DPPC is capable of having the hexagonal (H_{II}) arrangement partially, since the bilayer of phosphatidylethanolamine including less than 30 mol% phosphatidylcholine takes the hexagonal (H_{II}) arrangement [23]. This might be the case in the appearance of region C in the ripple structure. On the other hand, the density of acyl chains is tight in the region denoted D because of the convex curvature of the lower layer, so the motion of acyl chains is restrained; this region might then become an ordered one. In the regions denoted A or B in Fig. 8, the bilayer surface has a small curvature. Thus, these regions do not seem to be disordered as does region C.

Acknowledgement

We wish to thank Dr. K. Ohki for stimulating discussions.

References

1 Hubbell, W.L. and McConnell, H.M. (1971) J. Am. Chem. Soc. 93, 314–326.
2 Hemminga, M.A. (1983) Chem. Phys. Lipids 32, 323–383.
3 Marsh, D., Watts, A. and Knowles, P.F. (1977) Biochim. Biophys. Acta 465, 500–514.
4 Lange, A., Marsh, D., Wassmer, K.H., Meier, P., Kothe, G. (1985) Biochemistry 24, 4383–4392.
5 Zimm, B.H. and Bragg, J.K. (1959) J. Chem. Phys. 31, 526–535.
6 Wittebort, R.J., Schumidt, C.F. and Griffin, R.G. (1981) Biochemistry 20, 4223–4228.
7 Falkovitz, M.S., Seul, M. Frisch, H.L. and McConnell, H.M. (1982) Proc. Natl. Acad. Sci. USA 79, 3918–3921.
8 Schneider, M.B., Chan, W.K. and Webb, W.W. (1983) Biophys. J. 43, 157–165.
9 Egret-Charlier, M., Sanson, A. and Ptak, M. (1978) FEBS Lett. 89, 313–316.
10 Fernández, M.S. and Fromherz, P. (1977) J. Phys. Chem. 81, 1755–1761.
11 Griffith, O.H. and Jost, P.C. (1976) in Spin Labeling. Theory and Applications, Vol. 1 (Berliner, L.J., ed.), pp. 453–523, Academic Press.
12 Gaffney, B.J. (1976) in Spin Labelling. Theory and Applications, Vol. 1 (Berliner, L.J., ed.), pp. 567–571, Academic Press, New York.
13 Gaffney, B.J. and McConnell, H.M. (1974) J. Magn. Reson. 16, 1–28.
14 Hinz, H.J. and Sturtevant, J.M. (1972) J. Biol. Chem. 247, 6071–6075.
15 Shimshick, E.J. and McConnell, M.H. (1973) Biochemistry 12, 2351–2360.
16 Poinaszek, C.F., Marsh, D. and Smith, I.C.P. (1981) J. Magn. Reson. 43, 54.
17 Meier, P., Ohmes, E. and Kothe, G. (1986) J. Chem. Phys. 85, 3598–3614.
18 Müller, H.J., Luxnat, M. and Galla, H.J. (1986) Biochim. Biophys. Acta 856, 283–289.
19 Tsuchida, K., Hatta, I., Imaizumi, S., Ohki, K. and Nozawa, Y. (1985) Biochim. Biophys. Acta 812, 294–254.
20 Tsuchida, K., Ohki, K., Sekiya, T., Nozawa, Y. and Hatta, I. (1987) Biochim. Biophys. Acta 898, 53–58.
21 Larsson, K. (1977) Chem. Phys. Lipids 20, 225–228.
22 Meier, P., Blume, A., Ohmes, F.A., Neugebauer, F.A. and Koth, G. (1982) Biochemistry 21, 526–533.
23 Cullis, P.R. and De Kruijff, B. (1979) Biochim. Biophys. Acta 559, 399–420.